PHARMACIA

Pharmacia 72: 1–10
DOI 10.3897/pharmacia.72.e160847

Research Article

Comprehensive molecular docking, cytotoxicity, and ADMET analysis of documented curcuminoid derivatives on the A549 cell line

Mustafa Q. Alderawy[1], Mustafa M. AL-Hakiem[1], Reham A. AL-Anssari[2], Rita S. Elias[1]

1 *Department of Pharmaceutical Chemistry, College of Pharmacy, University of Basrah, Basrah, Iraq*
2 *Department of Pharmacognosy and Medicinal Plant, College of Pharmacy, University of Basrah, Basrah, Iraq*

Corresponding author: Mustafa Q. Alderawy (phmq89@gmail.com)

Received 2 June 2025 ♦ **Accepted** 25 July 2025 ♦ **Published** 12 August 2025

Citation: Alderawy MQ, AL-Hakiem MM, AL-Anssari RA, Elias RS (2025) Comprehensive molecular docking, cytotoxicity, and ADMET analysis of documented curcuminoid derivatives on the A549 cell line. Pharmacia 72: 1–10. https://doi.org/10.3897/pharmacia.72.e160847

Abstract

Various novel curcuminoids (1–7) and pyrazole derivatives of curcuminoids (8–14) were synthesized and characterized using spectrum analysis. The compounds produced were evaluated for antiproliferative effects against the A549 lung cancer cell line. Compound 2 exhibited notable cytotoxicity at 10.38 µg/mL, whereas compounds 4, 5, and 7 showed considerable cytotoxicity, with IC_{50} concentrations of 47.1, 23.4, and 82.4 µg/mL, respectively. Conversely, the other synthesized compounds exhibited only modest cytotoxicity. Moreover, *in silico* molecular docking analyses of EGFR (PDB ID: 4HJ0) demonstrated that compounds 2 and 6 displayed the lowest binding energies, −11.52 kcal/mol and −11.47 kcal/mol, respectively, indicating a higher affinity for the active pocket of the receptor, characterized by robust hydrogen bond interactions. Compound 12 had the highest binding energy (−8.42 kcal/mol) and the weakest affinity (KI = 670.04 nM). SwissADME analysis revealed satisfactory drug-likeness among all compounds, with no violations of Lipinski's rules and modest synthetic accessibility. ProTox-II indicated tolerable oral toxicity (LD_{50}: 1300–4000 mg/kg), although elevated immunotoxicity scores imply the need for additional safety assessment. These data identify compound 2 as a promising candidate for future optimization and preclinical development.

Keywords

Curcuminoid derivatives, A549 cell line, molecular docking, cytotoxicity, ADMET profiling

Introduction

Currently, cancer poses a significant public health issue, and cancer of the lungs is the most common type of malignant tumor. Lung malignancy is classified histologically into two types: non-small-cell lung cancer (NSCLC) and small-cell lung carcinoma (SCLC). The former accounts for approximately 80% of cases and has a very poor survival rate due to resistance to adjuvant chemotherapy (Jemal et al. 2011).

The abundance of natural chemicals derived from plants with effective tumor treatment capabilities has garnered global interest, owing to their accessibility and comparatively lower toxicity than conventional chemotherapy. Curcumin, a liposoluble polyphenol pigment extracted from the rhizomes of *Curcuma*, is a well-known nutritional supplement with a rich history. It is recognized for its diverse biological activities, including anti-inflammatory, anticoagulant, hypolipidemic, antioxidant, reactive

oxygen species scavenging, and anti-atherosclerotic properties, and is considered one of the key active ingredients in Chinese medicine due to its primary effective components (Gupta et al. 2013). However, the practical application of curcumin in medicine is limited by its poor water solubility, rapid metabolic degradation, and potential cytotoxicity to non-cancerous cells. Consequently, considerable attention has been directed toward exploring novel chemically synthesized curcumin analogues with comparable biological properties. Several recent studies have investigated the effects of curcumin compounds or derivatives on inhibiting the growth of cancer cells (Wu et al. 2015; Zhou et al. 2018; Chainoglou and Hadjipavlou-Litina 2019; Ali et al. 2021).

In recent years, several curcumin compounds have demonstrated strong antitumor efficacy (Tomeh et al. 2019). These are complex molecules with multiple pathways that may mediate chemotherapeutic and chemopreventive effects in cancer. They are also associated with a low risk of adverse effects. Moreover, curcumin interferes with several cellular signaling pathways, including angiogenesis, cell proliferation, inflammation, and programmed cell death (Sandur et al. 2007; Liang et al. 2008, 2009; Xu et al. 2013). Under laboratory conditions, curcuminoid derivatives have also been shown to inhibit the proliferation of several cancer cell lines, particularly in lung cancer (Watson et al. 2010; Chang et al. 2012; Liu et al. 2016).

These data strongly suggest potential clinical applicability in cancer control. Pyrazole and its derivatives constitute a highly significant group of heterocyclic compounds in pharmacology. Substituted pyrazoles have demonstrated diverse pharmacological activities, including anticancer effects. Certain pyrazole-based cytotoxic agents also exhibit chemopreventive properties (Xia et al. 2008; Al-Warhi et al. 2023).

The present study aimed to evaluate the cytotoxic properties of curcuminoid variants against a lung cancer cell line (A549), along with ADMET prediction. A molecular docking study was also conducted to elucidate their activity.

Experimental section

Chemical synthesis

Previously, curcuminoids (compounds 1–7) and pyrazole derivatives of curcuminoids (compounds 8–14) were synthesized and documented (AL-Hakiem et al. 2024), as shown in Figs 1, 2.

Preliminary cytotoxicity screening

An *in vitro* preliminary screening of the anticancer activity of curcuminoids 1–7 and pyrazole derivatives (8–14) against the A549 lung cancer cell line was conducted at the Department of Zoology and Cytology, Government College University, Faisalabad, Pakistan. The screening was performed using the MTT colorimetric assay (Mosmann 1983). A549 cells were cultured and then treated with a solution containing curcuminoids and pyrazole analogs (1–14) at a concentration of 0.4 mg/mL, dissolved in DMSO. The experiment was conducted in triplicate. The control group consisted of cancer cells treated with DMSO alone. After a 48-hour incubation at 37 °C and 5% CO_2, the cells were rinsed with phosphate-buffered saline to remove dead cells and cellular debris. Subsequently, the cells were exposed to a solution containing 0.5 mg/mL MTT and incubated for an additional 4 hours at 37 °C and 5% CO_2 until formazan crystals formed. The resulting crystals were dissolved in DMSO, and the absorbance of the solution was measured at a wavelength of 570 nm.

Calculation of the IC_{50} value of the active compounds

In this step, the IC_{50} value was determined for the compounds that demonstrated significant curative effects on the A549 cell line in the previous phase. This was accomplished by evaluating the impact of varying concentrations (25, 50, 100, 200, 400 μg/mL) of those compounds on the viability of lung cancer cells. The MTT assay was used to assess their effect. The data were analyzed, and the IC_{50} values were computed using GraphPad Prism 8.1 software. The findings were presented as ± SEM, with a *p*-value of less than 0.0001.

Molecular docking study

Molecular docking models were conducted using AutoDock 4 to examine the binding interactions between the target protein (receptor) and the ligand monomers. The three-dimensional structure of the epidermal growth factor receptor (EGFR) protein (PDB ID: 4HJ0) was retrieved from the Protein Data Bank (PDB) in PDB format. The protein structure was preprocessed to remove water molecules, ions, and other heteroatoms. Polar hydrogen atoms and Kollman charges were added using AutoDockTools (ADT). The processed receptor file was saved in PDBQT format for docking trials. The ligand structures were prepared in PDB format. Gasteiger charges were assigned, and rotatable bonds were defined using AutoDockTools. The ligand files were then converted and saved in PDBQT format.

The receptor's binding site was determined using AutoDockTools. A grid box was defined to enclose the predicted binding region, with specific coordinates (x, y, z) and dimensions calibrated to encompass the active site. AutoDock 4 was executed using the corresponding DPF file to perform the docking simulations. The output was saved in a Docking Log File (DLG), which contained detailed results on binding energies and ligand conformations. The binding energy values (in kcal/mol) and optimal ligand conformations were extracted from the DLG file. The docking outcomes were visualized and analyzed using structural visualization tools to examine the interactions between the ligands and the receptor.

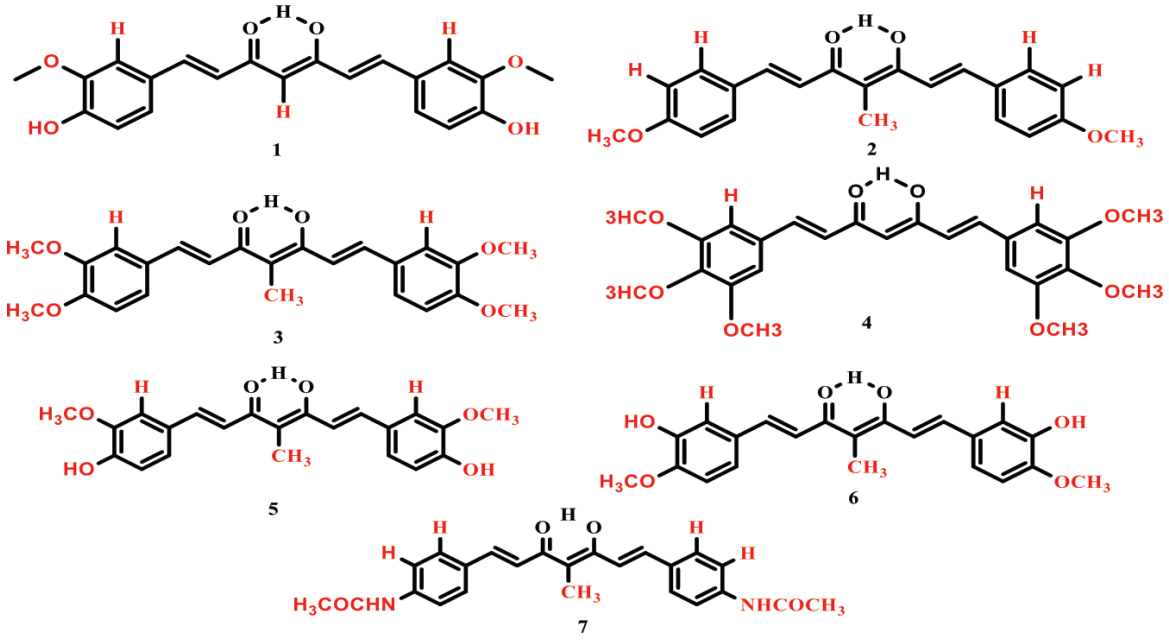

Figure 1. Chemical structure of curcuminoid compounds (1–7).

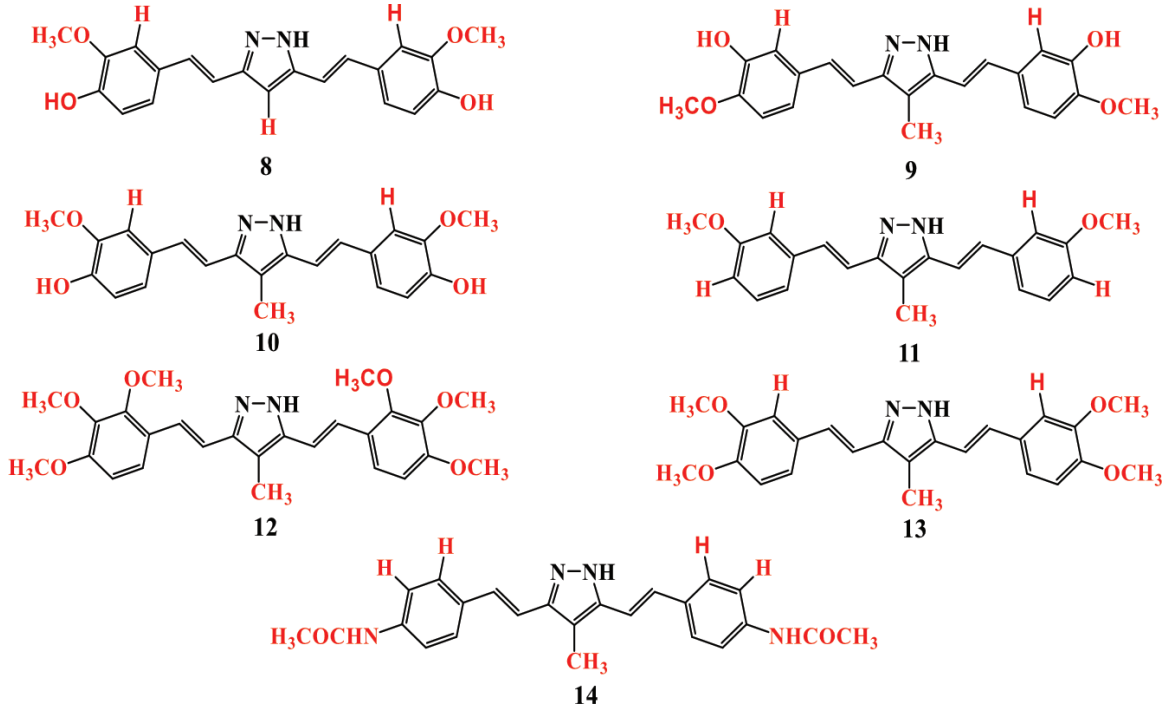

Figure 2. Chemical structure of pyrazole derivatives of curcuminoid compounds (8–14).

ADMET prediction

SwissADME (http://www.swissadme.ch) and ProTox-II (https://tox-new.charite.de/protox_II) were used to assess the pharmacokinetic and toxicity profiles of the compounds under study.

SwissADME analysis

We were provided with SMILES representations of all 14 compounds to evaluate their physicochemical properties and drug-likeness. The following parameters were extracted: Lipinski's Rule of Five, bioavailability score, PAINS (Pan Assay Interference Compounds), and synthetic accessibility. All data were downloaded in table format, manually sorted, and filtered to retain only pharmacologically relevant descriptors.

ProTox-II toxicity prediction

The same SMILES strings were submitted to the ProTox-II server to assess oral acute toxicity (LD_{50}, expressed in mg/kg), predicted toxicity class (I–VI), and probability-based predictions for hepatotoxicity, carcinogenicity, and immunotoxicity. The results were saved and used to interpret outcomes and prioritize compounds.

Results and discussion

Curcuminoids (compounds 1–7) and pyrazole derivatives of curcuminoids (compounds 8–14) demonstrated varying levels of cytotoxicity against the A549 cell line, with IC_{50} values ranging from 10 to 157 μg/mL.

Compound 2, a curcuminoid derivative, exhibited significant cytotoxicity (10.38 μg/mL) against the A549 cell line. In contrast, compound 8, a pyrazole derivative, displayed the strongest cytotoxicity within its group (59.23 μg/mL). Compounds 4, 5, and 7 also demonstrated notable cytotoxicity, with IC_{50} values of 47.1, 23.4, and 82.4 μg/mL, respectively. The remaining compounds exhibited only mild cytotoxicity.

The antiproliferative effects (IC_{50}) of the synthesized compounds on the A549 and HdFn cell lines are presented in Table 1 and illustrated in Figs 3, 4.

Table 1. Antiproliferative activity (IC_{50}) of synthesized compounds (1–14).

Compound	IC_{50} (A549) (μg/mL)	IC_{50} (HdFn) (μg/mL)
1	78.37	211
2	10.38	568
3	121.1	134.9
4	47.1	155.2
5	23.4	180.50
6	140.50	151.3
7	82.4	125.2
8	59.23	151.6
9	119	161.2
10	107.9	237.4
11	121.6	124.2
12	102.8	213.7
13	157.5	162.2
14	131.3	237.4

The selectivity index values for curcuminoid compounds (1–7) were 0.37, 0.02, 0.89, 0.30, 0.13, 0.93, and 0.66, respectively. For compounds 8–14, which are pyrazole derivatives of curcuminoids, the selectivity index values were 0.39, 0.74, 0.45, 0.97, 0.48, 0.09, and 0.55, respectively. None of the curcuminoid or pyrazole derivatives exhibited a selectivity index value greater than 3, the threshold for classification as highly selective. Table 2 summarizes the cytotoxicity and selectivity index values for the curcuminoid and pyrazole derivatives on the A549 cell line compared to the HdFn cell line (Weerapreeyakul et al. 2012).

Table 2. Classification of cytotoxicity and selectivity index (SI) of prepared compounds on the A549 cell line compared to the HdFn cell line.

Cytotoxicity	Selectivity index (SI) value	A549 vs. HdFn
Very strong cytotoxicity (IC50 < 10 μg/mL)	SI ≥ 3	–
Strong cytotoxicity (IC_{50} 10–100 μg/mL)	SI ≥ 3 SI < 3	Compounds (2, 5, 4, 8, 1, and 7)
Moderate cytotoxicity (IC_{50} 100–500 μg/mL)	SI ≥ 3 SI < 3	Compounds (12, 10, 9, 3, 11,14, 6, and 13)

The docking research findings, as presented in Table 3 along with Figs 5, 6, indicate that compound 2 exhibited the lowest binding energy (−11.52 kcal/mol) and the highest affinity (KI = 19.51 nM). Compound 6 also demonstrated low binding energy (−11.47 kcal/mol) and high affinity (KI = 3.93 nM). In contrast, compound 12 displayed the highest binding energy (−8.42 kcal/mol) and the lowest affinity (KI = 670.04 nM). Consequently, compound 2, which showed the highest affinity in the docking investigations, also exhibited the most potent antiproliferative effect in experimental analyses. This suggests that the strong binding affinity of this compound for the target receptor may contribute to its biological activity.

Table 3. AutoDock 4 results.

Compounds	Binding energy (kcal/mol)	Ki (nM)	H.B
1	-10.32	27.23	LYS721
2	-10.52	19.51	LYS721, MET769
3	-9.13	203.33	THR766, MET769, CYS773
4	-8.64	467.03	THR766, MET769
5	-10.57	17.78	MET769
6	-11.47	3.93	MET769, PHE832, THR766
7	-10.33	26.61	LYS721
8	-9.6	91.23	LYS721
9	-10.32	12.49	LYS692, LYS704, MET769
10	-10.41	23.51	LYS704, MET769, ASP831
11	-9.15	194.79	MET769
12	-8.42	670.04	LYS692, LYS721, MET769
13	-9.49	111.4	GLN767, MET769, ASP831
14	-9.86	58.85	MET769, THR766

Although compound 6 demonstrated significant affinity in docking experiments, its antiproliferative efficacy was limited. This discrepancy may be attributed to factors such as cell membrane permeability and compound stability within the intracellular environment. Compound 12, with the lowest affinity in docking studies, also showed the weakest antiproliferative effect, supporting the idea that receptor binding affinity is a critical factor in determining biological activity.

We used SwissADME and ProTox-II online tools to evaluate the ADMET and toxicity profiles of all 14 compounds studied (Tables 4, 5). This analysis was performed to support the molecular docking results targeting proteins associated with the A549 lung cancer cell line. The combined *in silico* study enabled an early assessment of pharmacokinetic viability and potential safety risks.

The *in silico* pharmacokinetic evaluation of the tested compounds using the SwissADME platform revealed favorable drug-like properties. All compounds exhibited a bioavailability score of 0.55, indicating a modest probability of achieving oral bioavailability. Importantly, none of the compounds violated Lipinski's Rule of Five, suggesting physicochemical features conducive to oral drug delivery. In addition, no PAINS (Pan Assay Interference Compounds) alerts were detected across the series, implying a low likelihood of false-positive results in biological assays.

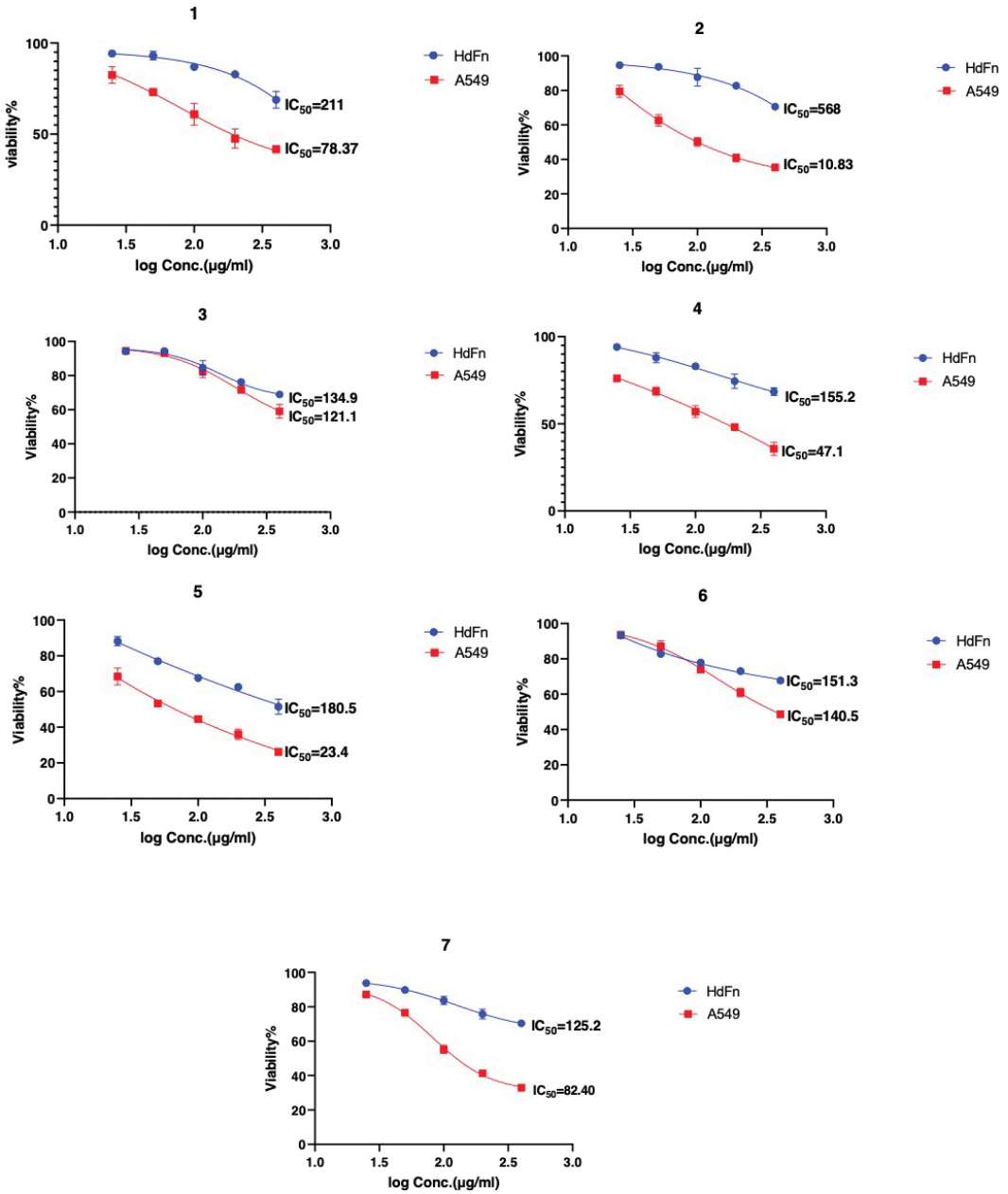

Figure 3. IC_{50} values of curcuminoid compounds (1–7) against A549 and HdFn cell lines.

Table 4. SwissADME results.

Compounds	Bioavailability score	Lipinski violations	PAINS alerts	Synthetic accessibility
1	0.55	0	0	2.97
2	0.55	0	0	3.32
3	0.55	0	0	3.47
4	0.55	0	0	3.74
5	0.55	0	0	3.35
6	0.55	0	0	3.51
7	0.55	0	0	3.35
8	0.55	0	0	2.98
9	0.55	0	0	2.9
10	0.55	0	0	3.42
11	0.55	0	0	3.04
12	0.55	0	0	3.51
13	0.55	0	0	3.27
14	0.55	0	0	3.55

The synthetic accessibility scores ranged from 2.9 to 3.74, suggesting a reasonable feasibility for chemical synthesis and scalability. Collectively, these results emphasize the pharmacological promise of the tested compounds and support their progression to experimental validation, particularly for the development of lung cancer therapeutics targeting the A549 cell line.

According to ProTox-II, all compounds were classified within toxicity classes 4 or 5.

The estimated LD_{50} values ranged from 1300 to 4000 mg/kg, suggesting a relatively safe toxicological profile and supporting the need for further investigation. Compounds 1–7 did not induce hepatotoxicity or carcinogenicity; however, they consistently affected immune function, indicating potential immunological disruption.

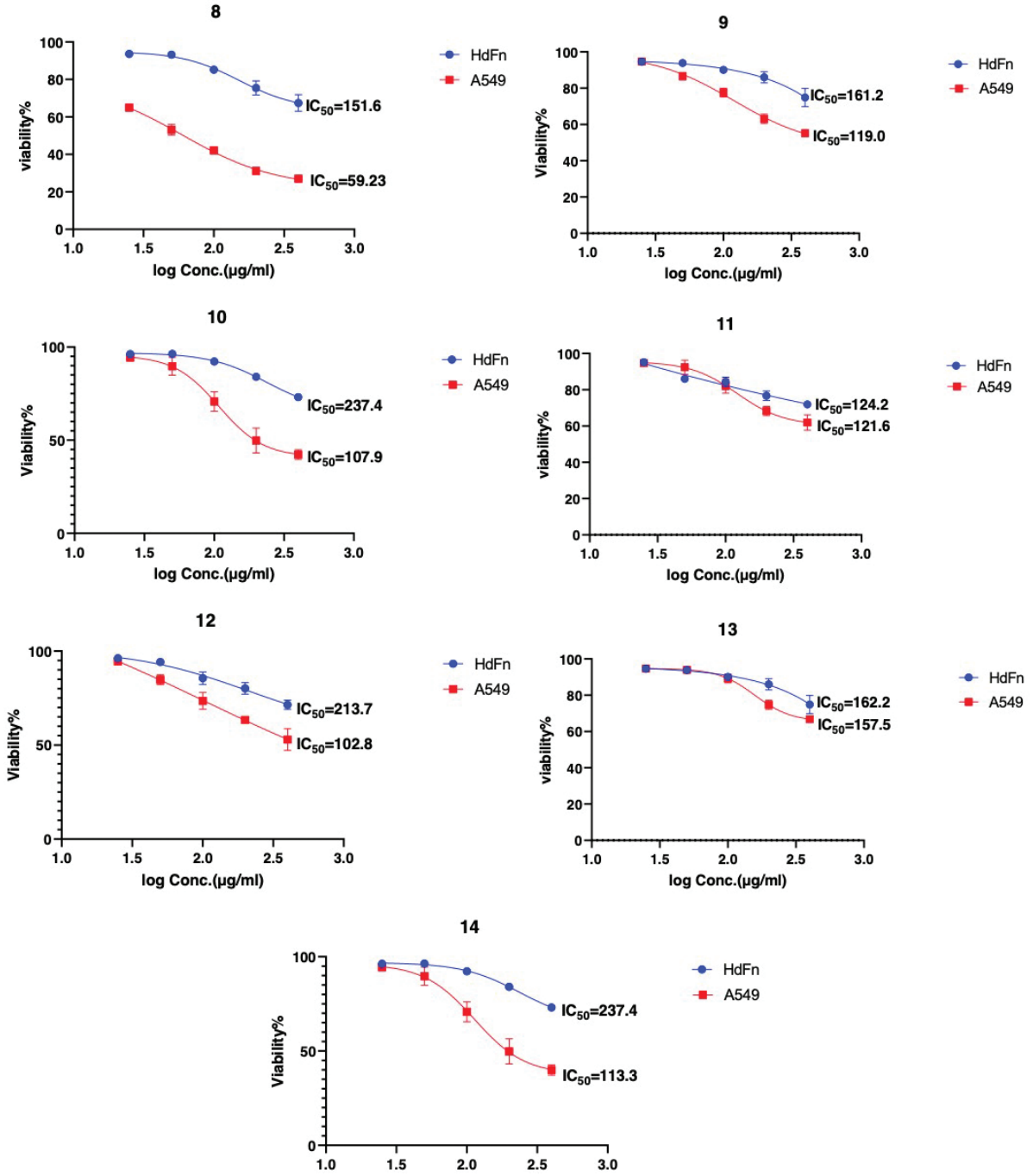

Figure 4. IC_{50} values of pyrazole derivatives of curcuminoid compounds (8–14) against A549 and HdFn cell lines.

Compounds 8–14 exhibited enhanced biological activity, with some classified as both hepatotoxic and carcinogenic (probability > 0.53). This may be attributed to the incorporation of 1,2,3-triazole and extended aromatic systems (Mardaneh et al. 2025). Immunotoxicity remained markedly high across all compounds (0.85–0.99), highlighting the presence of significant immunological associations that warrant additional scientific evaluation.

These results align with previous research emphasizing the anticancer efficacy of curcumin analogs on A549 cells. Wu et al. (2015) reported significant cytotoxicity for the curcumin derivative JZ534, with IC_{50} values comparable to those of compound 2 in the present study. Similarly, Zhou et al. (2018) demonstrated that MHMM-41, a novel curcumin-derived compound, induced ROS-mediated apoptosis in A549 cells. Compound 2 in this study exhibited enhanced efficacy, with an IC_{50} of 10.38 µg/mL and a strong binding affinity of −11.52 kcal/mol to EGFR. Moreover, Xu et al. (2013) and Mardaneh et al. (2025) showed that inhibition of EGFR by synthetic curcumin analogs is a key mechanism in suppressing lung cancer cell proliferation. These parallels support the conclusion that the investigated compounds—especially compound 2—have potential for further development as anticancer agents. The discrepancy between docking results and biological activity observed for compound 6 may be attributed to limitations in membrane permeability or intracellular stability, consistent with findings by Liu et al. (2016).

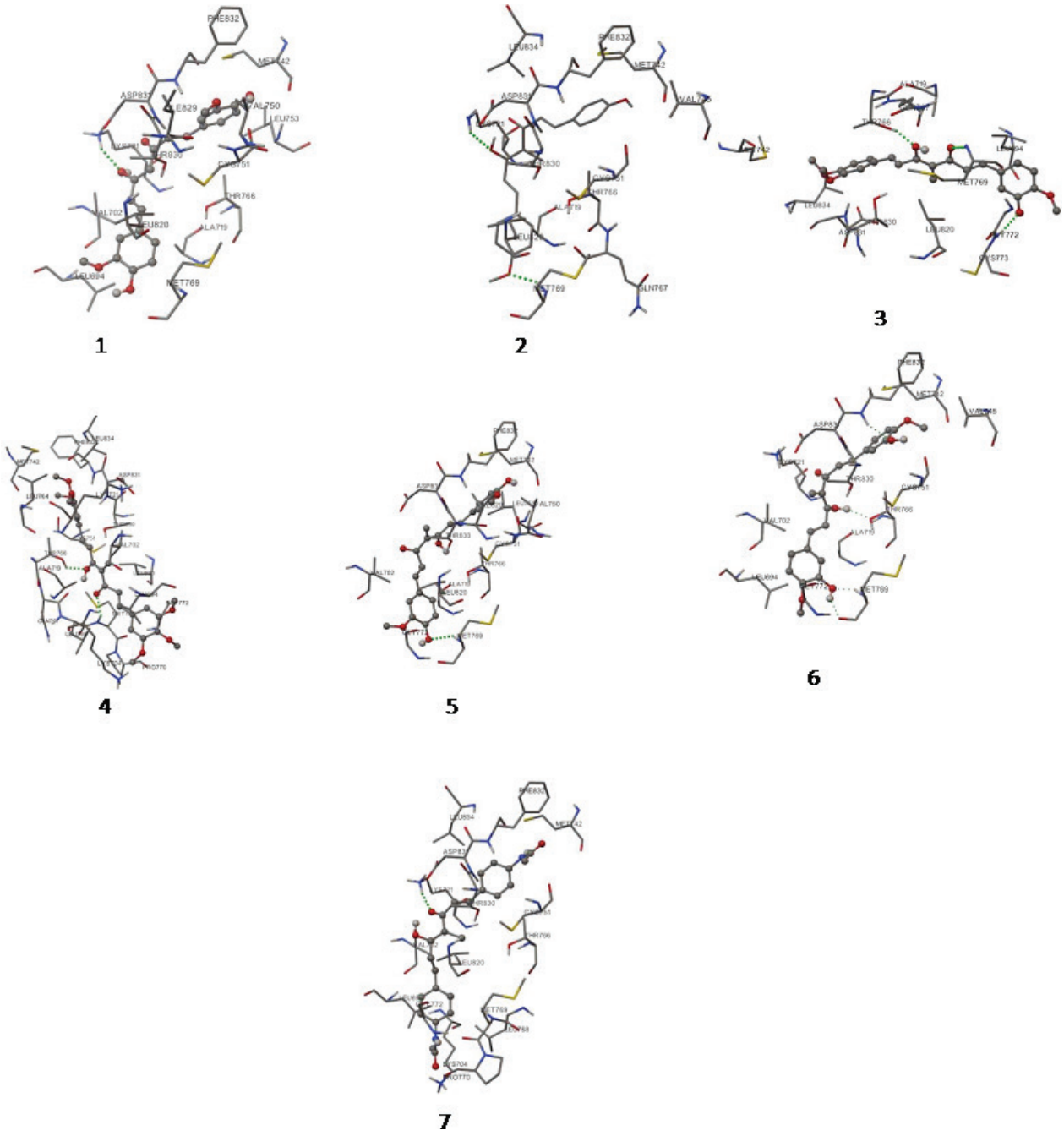

Figure 5. Molecular docking results of compounds (1–7).

Table 5. ProTox-II results.

Compounds	LD50 (mg/kg)	Toxicity class	Hepatotoxicity	Carcinogenicity	Immunotoxicity
1	2000	4	Inactive (0.61)	Inactive (0.84)	Active (0.92)
2	2000	4	Inactive (0.54)	Inactive (0.75)	Active (0.95)
3	4000	5	Inactive (0.54)	Inactive (0.75)	Active (0.99)
4	2000	4	Inactive (0.53)	Inactive (0.66)	Active (0.96)
5	4000	5	Inactive (0.60)	Inactive (0.82)	Active (0.98)
6	2000	4	Inactive (0.59)	Inactive (0.81)	Active (0.96)
7	2000	4	Inactive (0.56)	Inactive (0.65)	Active (0.98)
8	1314	4	Active (0.57)	Active (0.56)	Active (0.96)
9	1300	4	Active (0.56)	Active (0.61)	Active (0.98)
10	1300	4	Active (0.56)	Active (0.53)	Active (0.99)
11	1300	4	Active (0.55)	Active (0.54)	Active (0.99)
12	1300	4	Active (0.55)	Active (0.55)	Active (0.85)
13	1300	4	Active (0.56)	Active (0.53)	Active (0.99)
14	1300	4	Active (0.60)	Active (0.55)	Active (0.95)

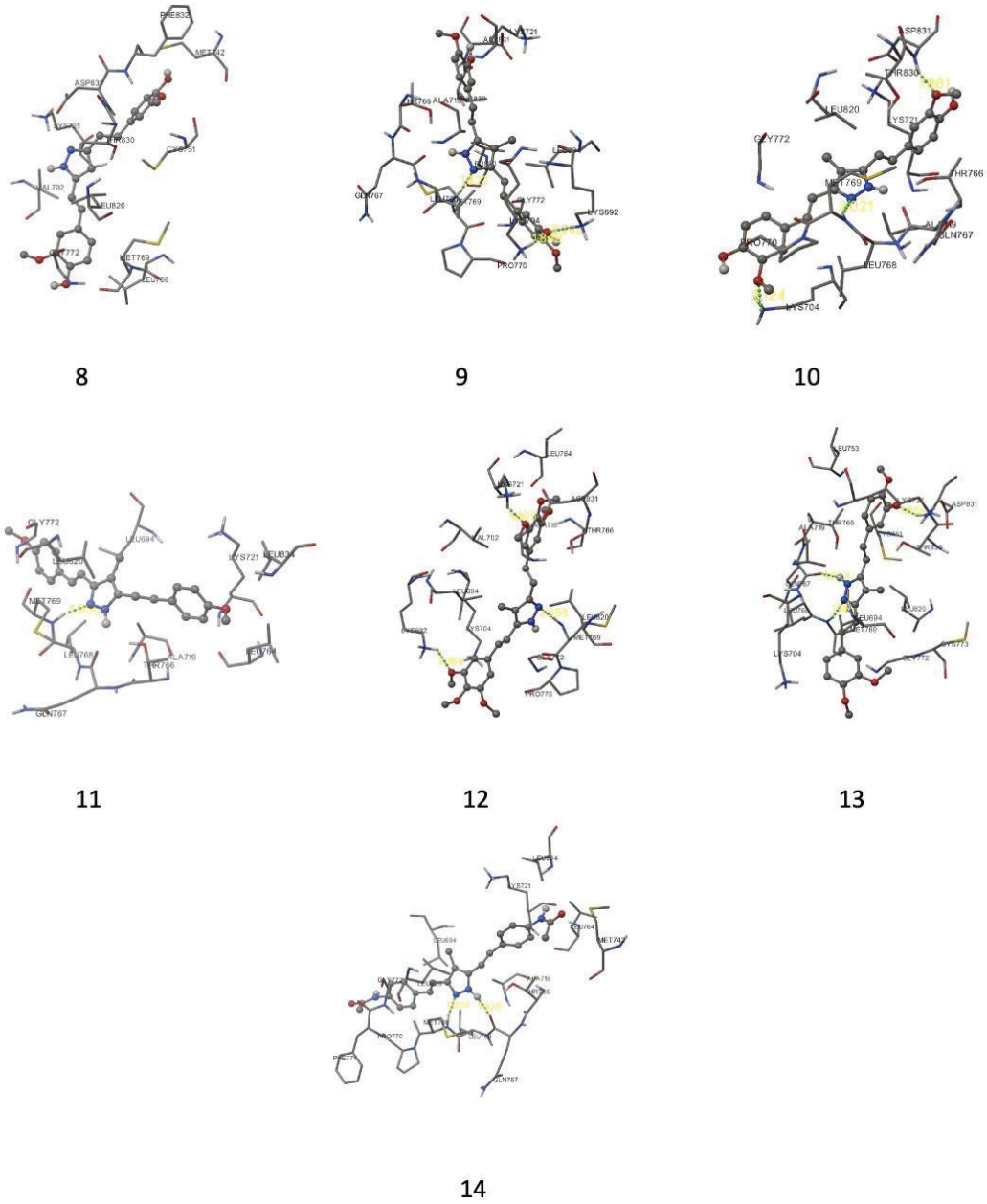

Figure 6. Molecular docking results of compounds (8–14).

Conclusion

This research integrated antiproliferative assays with molecular docking, as well as ADMET and toxicity prediction, to evaluate the synthesized compounds as potential anticancer agents. Compound 2 demonstrated the most potent antiproliferative activity along with high binding affinity, whereas compound 6 exhibited significant affinity but only moderate activity. Compound 12, which had the lowest binding affinity, also showed weak biological activity, reinforcing the correlation between binding affinity and biological efficacy. The SwissADME analysis confirmed favorable drug-likeness across all compounds, with no Lipinski violations, moderate synthetic accessibility, and absence of PAINS alerts. ProTox-II predicted tolerable oral toxicity; however, elevated immunotoxicity scores suggest that further safety evaluation is necessary. Taken together, these findings support compound 2 as a promising candidate for further optimization and preclinical development.

Additional information

Conflict of interest

The authors have declared that no competing interests exist.

Ethical statements

The authors declared that no clinical trials were used in the present study.

The authors declared that no experiments on humans or human tissues were performed for the present study.

The authors declared that no informed consent was obtained from the humans, donors or donors' representatives participating in the study.

The authors declared that no experiments on animals were performed for the present study.

Use of commercially available immortalised human and animal cell lines: A549 cell line was kindly provided by the Department of Zoology and Cytology, Government College University, Faisalabad, Pakistan..

Use of AI

No use of AI was reported.

Funding

No funding was reported.

Author contributions

Mustafa Q. Alderawy: Conceptualization, Molecular Docking, Writing – Original Draft. Mustafa M. Al-Hakiem: ADMET Analysis, Data Curation, Visualization. Reham A. Al-Ansari: Cytotoxicity Experiments. Rita S Elias: Methodology, Writing – Review & Editing.

Author ORCIDs

Mustafa Q. Alderawy https://orcid.org/0000-0001-5747-6614
Mustafa M. AL-Hakiem https://orcid.org/0000-0002-4400-4631
Reham A. AL-Anssari https://orcid.org/0000-0001-6880-2120
Rita S. Elias https://orcid.org/0000-0003-0910-9013

Data availability

All of the data that support the findings of this study are available in the main text or Supplementary Information.

References

Al-Hakiem MM, Alderawy MQ, Adnan R, Elias RS (2024) Synthesis, characterization, and antibacterial activity study of novel curcuminoids derivatives. Iraqi Journal of Pharmaceutical Sciences 33(1): 154–162. https://doi.org/10.31351/vol33iss1pp154-162

Al-Warhi T, El Kerdawy AM, Said MA, Albohy A, Elsayed ZM, Aljaeed N, Elkaeed EB, Eldehna WM, Abdel-Aziz HA, Abdelmoaz MA (2023) Novel 2-(5-Aryl-4,5-dihydropyrazol-1-yl) thiazol-4-one as EGFR inhibitors: synthesis, biological assessment and molecular docking insights. Drug Design, Development and Therapy 17: 1457–1471. https://doi.org/10.2147/DDDT.S356988

Ali A, Ali A, Tahir A, Bakht MA, Salahuddin, Ahsan MJ (2021) Molecular engineering of curcumin, an active constituent of Curcuma longa L. (Turmeric) of the family Zingiberaceae with improved antiproliferative activity. Plants 10(8): 1559. https://doi.org/10.3390/plants10081559

Chainoglou E, Hadjipavlou-Litina D (2019) Curcumin analogues and derivatives with anti-proliferative and anti-inflammatory activity: structural characteristics and molecular targets. Expert Opinion on Drug Discovery 14(8): 821–842. https://doi.org/10.1080/17460441.2019.1614560

Chang CC, Fu CF, Yang WT, Chen TY, Hsu YC (2012) The cellular uptake and cytotoxic effect of curcuminoids on breast cancer cells. Taiwanese Journal of Obstetrics and Gynecology 51(3): 368–374. https://doi.org/10.1016/j.tjog.2012.07.009

Gupta SC, Kismali G, Aggarwal BB (2013) Curcumin, a component of turmeric: from farm to pharmacy. Biofactors 39(1): 2–13. https://doi.org/10.1002/biof.1079

Jemal A, Bray F, Center MM, Ferlay J, Ward E, Forman D (2011) Global cancer statistics. CA: a cancer journal for clinicians 61(2): 69–90. https://doi.org/10.3322/caac.20107

Liang G, Li X, Chen L, Yang S, Wu X, Studer E, Gurley E, Hylemon PB, Ye F, Li Y, Zhou H (2008) Synthesis and antiinflammatory activities of mono-carbonyl analogues of curcumin. Bioorganic & Medicinal Chemistry Letters 18(4): 1525–1529. https://doi.org/10.1016/j.bmcl.2007.12.068

Liang G, Yang S, Zhou H, Shao L, Huang K, Xiao J, Huang Z, Xiaokun Li (2009) Synthesis, crystal structure and anti-inflammatory properties of curcumin analogues. European Journal of Medicinal Chemistry 44(2): 915–919. https://doi.org/10.1016/j.ejmech.2008.01.031

Liu D, You M, Xu Y, Li F, Zhang D, Li X, Hou Y (2016) Inhibition of curcumin on myeloid-derived suppressor cells is requisite for controlling lung cancer. International Immunopharmacology 39: 265–272. https://doi.org/10.1016/j.intimp.2016.07.035

Mardaneh P, Pirhadi S, Mohabbati M, Khoshneviszadeh M, Rezaei Z, Saso L, Edraki N, Omidreza Firuzin (2025) Design, synthesis and pharmacological evaluation of 1,4-naphthoquinone-1,2,3-triazole hybrids as new anticancer agents with multi-kinase inhibitory activity. Scientific Reports 15(1): 6639. https://doi.org/10.1038/s41598-025-87483-w

Mosmann T (1983) Rapid colorimetric assay for cellular growth and survival: application to proliferation and cytotoxicity assays. Journal of Immunological Methods 65(1–2): 55–63. https://doi.org/10.1016/0022-1759(83)90303-4

Sandur SK, Pandey MK, Sung B, Ahn KS, Murakami A, Sethi G, Limtrakul P, Badmae P, Bharat B, Aggarwal B (2007) Curcumin, demethoxycurcumin, bisdemethoxycurcumin, tetrahydrocurcumin and turmerones differentially regulate anti-inflammatory and anti-proliferative responses through a ROS-independent mechanism. Carcinogenesis 28(8): 1765–1773. https://doi.org/10.1093/carcin/bgm123

Tomeh MA, Hadianamrei R, Zhao X (2019) A review of curcumin and its derivatives as anticancer agents. International Journal of Molecular Sciences 20(5): 1033. https://doi.org/10.3390/ijms20051033

Watson JL, Greenshields A, Hill R, Hilchie A, Lee PW, Giacomantonio CA, Hoskin DW (2010) Curcumin- induced apoptosis in ovarian carcinoma cells is p53- independent and involves p38 mitogen- activated protein kinase activation and downregulation of Bcl- 2 and survivin expression and Akt signaling. Molecular Carcinogenesis: Published in cooperation with the University of Texas MD Anderson Cancer Center 49(1): 13–24. https://doi.org/10.1002/mc.20571

Weerapreeyakul N, Nonpunya A, Barusrux S, Thitimetharoch T (2012) Evaluation of the anticancer potential of six herbs against a hepatoma cell line. https://doi.org/10.1186/1749-8546-7-15

Wu J, Cai Z, Wei X, Chen M, Ying S, Shi L, Xu RA,He F, Liang G, Zhang X (2015) Anti-lung cancer activity of the curcumin analog JZ534 in vitro. BioMed Research International 2015. https://doi.org/10.1155/2015/504529

Xia Y, Fan CD, Zhao BX, Zhao J, Shin DS, Miao JY (2008) Synthesis and structure–activity relationships of novel 1-arylmethyl-3-aryl-

1H-pyrazole-5-carbohydrazide hydrazone derivatives as potential agents against A549 lung cancer cells. European Journal of Medicinal Chemistry 43(11): 2347–2353. https://doi.org/10.1016/j.ejmech.2008.01.021

Xu YY, Cao Y, Ma H, Li HQ, Ao GZ (2013) Design, synthesis and molecular docking of α, β-unsaturated cyclohexanone analogous of curcumin as potent EGFR inhibitors with antiproliferative activity. Bioorganic & Medicinal Chemistry 21(2): 388–394. https://doi.org/10.1016/j.bmc.2012.11.031

Zhou GZ, Li AF, Sun YH, Sun GC (2018) A novel synthetic curcumin derivative MHMM-41 induces ROS-mediated apoptosis and migration blocking of human lung cancer cells A549. Biomedicine & Pharmacotherapy 103: 391–398. https://doi.org/10.1016/j.biopha.2018.04.086

Supplementary material 1

Additional figure

Authors: Mustafa Q. Alderawy, Mustafa M. AL-Hakiem, Reham A. AL-Anssari, Rita S. Elias

Data type: docx

Link: https://doi.org/10.3897/pharmacia.72.e160847.suppl1